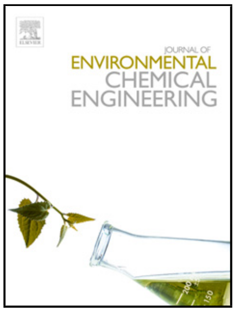

Treatment of real non-biodegradable wastewater: Feasibility analysis of a zero-valent iron/H_2O_2 process

Pamela Belén Ramos (Investigation) (Conceptualization) (Methodology) (Writing - original draft), Paula Vitale (Investigation) (Writing - review and editing) (Formal analysis), Gastón Pablo Barreto (Supervision), Francisca Aparicio (Investigation), María de los Ángeles Dublan (Investigation), Gladys Nora Eyler

PII: S2213-3437(20)30302-X
DOI: https://doi.org/10.1016/j.jece.2020.103954
Reference: JECE 103954

To appear in: *Journal of Environmental Chemical Engineering*

Received Date: 26 December 2019
Revised Date: 10 April 2020
Accepted Date: 13 April 2020

Please cite this article as: Ramos PB, Vitale P, Barreto GP, Aparicio F, de los Ángeles Dublan M, Eyler GN, Treatment of real non-biodegradable wastewater: Feasibility analysis of a zero-valent iron/H_2O_2 process, *Journal of Environmental Chemical Engineering* (2020), doi: https://doi.org/10.1016/j.jece.2020.103954

Treatment of real non-biodegradable wastewater: Feasibility analysis of a zero-valent iron/H_2O_2 process.

Pamela Belén Ramos[1], Paula Vitale[1], Gastón Pablo Barreto[1], Francisca Aparicio[2], María de los Ángeles Dublan[3], Gladys Nora Eyler[1].*

[1]Center for Research in Physics and Engineering of the Center of Buenos Aires Province, CIFICEN (UNCPBA-CONICET-CICPBA). Pinto 399, B7400JWI, Olavarría, Buenos Aires, Argentina.

[2]Instituto de Investigaciones Fisicoquímicas Teóricas y Aplicadas (INIFTA), Departamento de Química, Facultad de Ciencias Exactas, Universidad Nacional de la Plata, CONICET. Casilla de Correo 16, Sucursal 4, 1900 La Plata, Argentina.

[3]Centro Regional de Estudio Sistémico de las Cadenas Agroalimentarias de la Facultad de Agronomía de la UNCPBA. Rep. de Italia 780. Azul, Buenos Aires, Argentina.

**E-mail address: pamela.ramos@fio.unicen.edu.ar*

Graphical abstract

Highlights

- Treatment of real non-biodegradable textile effluent applying Advanced Oxidation Technologies (AOTs).
- The degradation kinetics was investigated in laboratory and pilot scale.
- The CSW/H_2O_2 degradation process is an economically viable and environmentally friendly option.
- Catalytic use of commercial steel wool as a source of zero-valent iron.
- The use of a metallurgical waste as a source of iron reaches degradations of 87%

Abstract

Textile industries present notable environmental problems related mainly to the use and management of water resources. The application of advanced oxidation technologies (AOT) to a real and complex system was analyzed. The degradation of a real textile effluent in the presence of commercial steel wool (CSW, zero-valent iron) and H_2O_2 as oxidant was studied. The effects of H_2O_2 concentration (0-0.08 mol L^{-1}), mass of CSW (0-0.4 g L^{-1}) and temperature (15-45 °C) on the reduction of the chemical oxygen demand (COD) of the textile effluent were evaluated. Kinetic studies were performed at laboratory and pilot scales at different temperatures under optimal conditions (0.037 mol L^{-1} of H_2O_2 and 0.247 g L^{-1} of CSW). Iron species (Fe^{2+}, Fe^{3+}, total Fe) were quantified in solution for different experiments as a function of time. COD reductions of 87.69% at lab scale and 89.55% at optimized pilot scale in 300 min (140.66 mgO_2 L^{-1} of COD, final discharge) were obtained. A metallurgical residue was tested as iron source, obtaining high COD removal (65%). Operating costs were calculated. Phytotoxicity tests performed before and after treatment showed that the effluent treated under optimal conditions was non-toxic.

Keywords: *wastewater, degradation, Advanced Oxidation Technologies (AOT), zero-valent iron, phytotoxicity tests.*

1. Introduction

The development of the consumer society has led to an increase in industrial activity and, consequently, to the production of large amounts of chemical compounds that pollute the environment and persist in waterways. Among the different types of pollution sources, those of anthropogenic-industrial origin usually have an important impact on the environment where the industries are located. The inadequate use of water can transform this non-renewable resource into a waste. In the last decades, the effects of pollution on health and the associated ecological risks have encouraged the development of new technologies for the remediation and treatment of wastewater [1]. The textile industry presents notable environmental challenges linked mainly to the use and management of water resources, requiring large amounts of drinking water and groundwater in its processes, and with textile wastewater being one of the most polluting of all industrial sectors [2]. These wastewaters are characterized by high COD (40-7000 mg L^{-1}), large variety of organic compounds, low biodegradability with BOD_5/COD ratios close to 0.25, BOD_5 values between 80 and 6000 mg L^{-1}, strong color, unstable pH, suspended solids, and salinity [3-9]. Once treated, textile waters are usually discharged to the sewer.

The need for a rational use of the limited water resources has encouraged over the last few decades the introduction of increasingly restrictive laws that require different manufacturing industries to apply efficient treatments to their effluents for later discharge. This has forced the research and development of treatment technologies for water used in industrial applications [10].

Most of the organic compounds found in industrial effluents are resistant to conventional methods of chemical and biological treatments [11-15]. Therefore, alternative systems are being studied, in particular photochemical and photocatalytic processes. In this context, treatments known as Advanced Oxidation Technologies (AOTs) that allow the conversion of organic pollutants with a wide variety of structures into substances of lower toxicity and greater biodegradability have been investigated [7-10].

AOTs are based on physicochemical processes capable of producing fundamental changes in the chemical structure of the pollutants through in situ generation of highly reactive and highly oxidizing radical species (HO•) obtained from homogeneous and heterogeneous catalytic processes [10]. The Fenton process is one of the most commonly applied mechanisms in the degradation of different effluents through the generation of HO• radicals from the reaction of hydrogen peroxide and Fe^{2+} ions in aqueous solution at acidic pH [16-19]. In addition to its ability to degrade non-biodegradable compounds, this process can reduce effluent toxicity and remove color [20, 21]. These characteristics make Fenton processes especially interesting for the advanced treatment of textile industry wastewaters and have driven its growing development and application at industrial scale during the last two decades.

Recent studies have revealed that organic dyes can be efficiently degraded by AOTs [22, 23], and these kind of processes can be effective for decolorization, COD reduction, and mineralization of real effluents in short irradiation time [24-26]. In addition, many studies have also developed combined AOP and biological systems for the treatment of a diversity of industrial wastewater [12, 27].

Various degradation treatments applying different AOTs on recalcitrant organic substances by have been studied; however, few studies have been carried out with real wastewater (complex, non-simulated systems) from the finishing stages of textile industries [12, 28-30].

In this work, the degradation process of a real textile effluent involving a treatment with Commercial Steel Wool (CSW) and H_2O_2 was studied. The degradation kinetics was studied both at laboratory and pilot scale, obtaining the rate constants (k_{deg}) for different conditions. This kinetics analysis can be useful for making decisions respect to the variables modification during the dradation process. In addition, the efficiency of using a metallurgical waste from a turning industry was also evaluated, giving value to this waste and reintroducing it into the production system. The technical, environmental and economic feasibility of the proposed treatment system was analyzed.

2. Experimental

2.1. Real textile effluent and sampling

A real textile effluent was obtained from a denim-jeans dyeing and finishing plant located in the Buenos Aires province, Argentina. This plant has a daily production of approximately 3600 articles of clothing and 250 m^3 of effluent. Currently, the company carries out a flocculation-coagulation process that does not allow to compliance with the discharge parameters of the Argentine legislation. The effluent consisted of dyes and finishing products, with a high COD (1500 mg L^{-1}) and solid content (3.5 mg L^{-1}) and low biodegradability (0.05). The pH was 7.2 and it had a blue color. The effluent samples were not diluted and were initially filtered to remove suspended solids (abrasive materials and lint). The initial pH was not adjusted at the beginning of the experiment. The samples were taken randomly in June and December 2017 due to the variability in the composition of the effluent according to production requirements. The filtered effluent was homogenized and stored at 4 °C to minimize any further bacterial processes [31].

2.2. Iron source and characterization

The morphology of 0.5 cm-long fragments of CSW was analyzed by scanning electron microscopy (SEM) (Carl Zeiss, MA10). The filaments were ca. 40 μm wide and 8 μm thick, with a nonporous surface (Figure 1a) [32].

Energy dispersive X-ray spectroscopy (EDS) (Oxford, INCA Energy 250) was used to determine the semi-quantitatively elemental composition (w/w). The data were obtained over 25 different points of the CSW surface. As expected for typical low carbon steel, the most abundant components were Fe (84.9 %W) and C (12.93 %W).

The diffractogram corresponding to the iron source (CSW) is shown in Figure 1b. The characteristic peaks of the Fe° phases (cubic system) are clearly visible, while no oxides were detected. The peaks at 45.14 ° and 65.76 ° correspond to the planes (0 1 1) and (0 0 2) respectively [32].

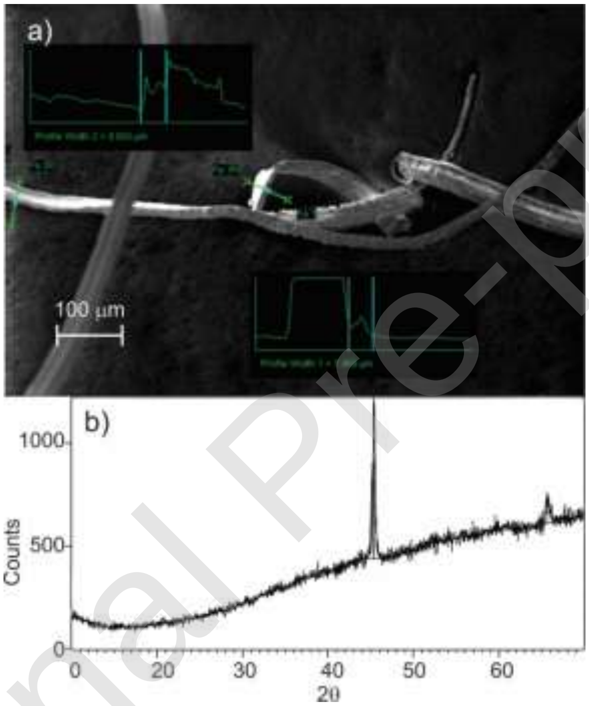

Figure 1. a) SEM micrograph of the surface of CSW at 200X magnification, 20 kV. **b)** X-ray diffractogram of CSW.

2.3. Materials and experimental procedure

Hydrogen peroxide (20 mol L^{-1}, Merck) was used as oxidizing agent and commercial steel wool (CSW) was used as source of Fe^{2+} and Fe^{3+}. All chemicals used were at least of reagent grade and were used as received without further purification.

A cylindrical 50 mL laboratory reactor with temperature control was used for the lab-scale degradation of the real textile effluent. The treatment consisted in the addition of H_2O_2 (oxidizing agent) and CSW to the filtered textile effluent. The temperature was controlled between 15±2 °C and 45±2 °C with a thermostatic water bath.

For the pilot scale tests, a 5 L batch reactor with a different configuration was used. In that case, the CSW was placed in a packed bed, as shown in Figure 2.

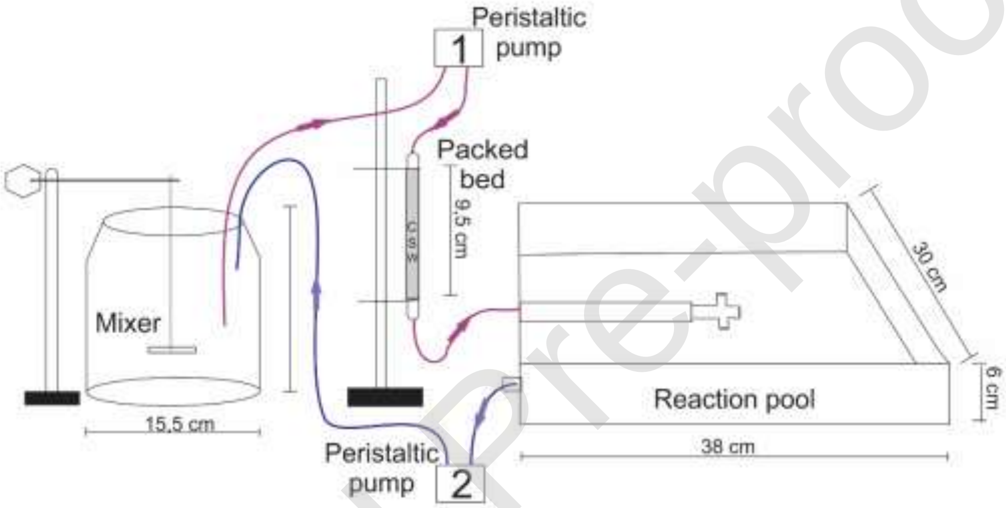

Figure 2. Schematic diagram of the pilot-scale experimental system with a CSW packed bed.

H_2O_2 and CSW were used in optimal amounts as determined by an experimental model: 0.037 mol L^{-1} of H_2O_2 and 0.247 g L^{-1} of CSW at room temperature (*ca*. 15 °C) [33]. The degradation process was monitored by measuring COD, Fe^{2+}, Fe^{3+} and pH every 300 min. All the tests were performed in triplicate. COD and pH were measured periodically during effluent storage to ensure that no degradation of the samples occurred.

2.4. Analyses

The standard methodologies established by the American Public Health Association (APHA 2005) for the determination of each physicochemical parameter value were used. A portable pH-meter was used to measure the pH of the solution (model AD100, ADWA). A Carl Zeiss microscope (model MA10) with an associated EDS detector (Oxford, model INCA Energy 250) was used to study the morphology and composition of the CSW used in the degradation process. A diffractometer (Panalytical, Empyrean model) with PIXCEL3D detector was used to detect the components and phases present in the CSW. Residual Fe^{2+} in the solution was measured through the characteristic wavelength of 512 nm corresponding to the complex of *o*-phenanthroline with Fe^{2+} using a UV–Vis spectrophotometer (Mapada, UV-1800PC) [34]. For the determination of total iron, the same technique was applied to the sample previously treated with a reducing agent (10% hydroxylamine chloride).

COD reduction (%) was measured at 300 min of reaction at a wavelength of 600 nm using a Mapada UV-1800PC spectrophotometer and a HANNA thermo-reactor. Total organic carbon (TOC) was determined with a high-temperature carbon analyzer (Shimadzu, TOC-5000A) using a calibration curve with potassium biphtalate standard. Standard solutions were run before each analysis to check for instrumental shifts.

The global degradation kinetics was studied by applying a pseudo-first order treatment. The degradation rate constants (k_{deg}) were obtained from plots of ln (COD_f/COD_i) as a function of time.

2.5. Phytotoxicity tests

Dilutions of the textile effluent at different percentages (100%, 25% and 12.5% final concentration) were used for the phytotoxicity analyses. The plant species used were: lettuce (*Lactuca sativa* L., criolla variety) obtained from the PRO-Huerta INTA program, and radish (*Raphanus sativus*), pound pink body with white tip obtained from La Germinadora.

The tests were carried out using the method proposed by Navarro et al. [35] with modifications. A filter paper disc was placed in Petri dishes with 1 g of cotton, autoclaved for 20 min at 121 °C and dried in an oven before the tests. For each plant species, 5 mL of effluent (concentrated or diluted) was added to the Petri dishes in triplicate, placing 20 seeds per plate. The plates with lettuce seeds were incubated for 120 h in the dark at 20±1 °C, while the plates with radish seeds were incubated for 120 h in the dark at 27±1 °C. Plates with 5 mL of sterile distilled water were used as control. For the incubation, the plates were placed in plastic bags to reduce moisture loss.

The effect on the germinative power and root elongation of the seeds of each species was analyzed by determining the relative growth index (RGI). The root elongation data were analyzed using the Kruskal-Wallis statistical test and Dunn’s multiple comparison test [36].

3. Results and discussions

3.1. Effect of the treatment variables

3.1.1. Effect of H_2O_2 concentration

In Figures 3 a and b, the COD reduction (%) of the effluent and the variation in Fe^{2+} concentration after 300 min of treatment at different initial concentrations of H_2O_2 are shown, respectively. Hydrogen peroxide concentration was varied between 0.00 and 0.08 mol L^{-1} while maintaining the amount of added CSW at 0.2 g L^{-1}.

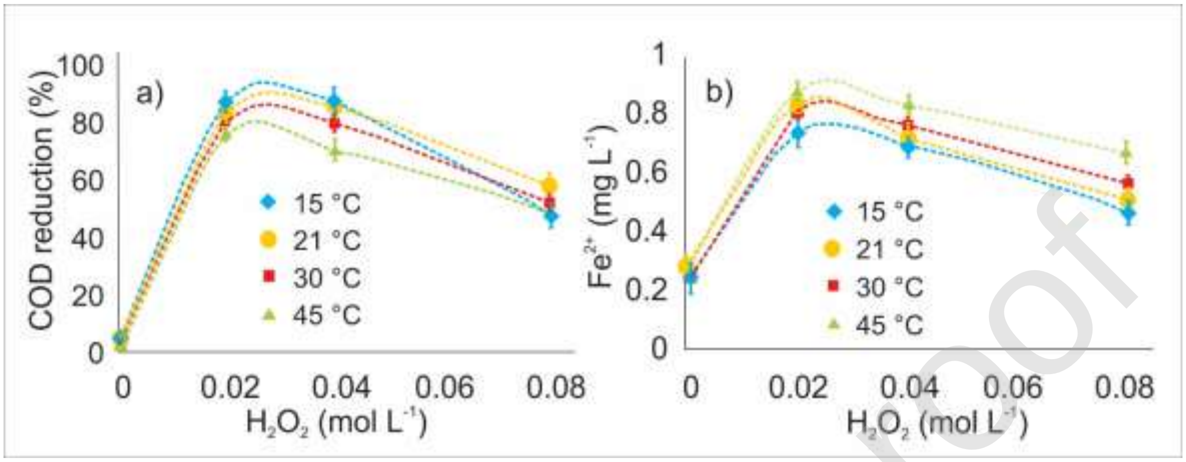

Figure 3. **a)** Effect of H_2O_2 concentration on COD reduction (%), experimental conditions: 0.2 g L^{-1} of CSW, time=300 min and initial effluent pH, **b)** Effect of H_2O_2 concentration on Fe^{2+} profiles, experimental conditions: 0.2 g L^{-1} of CSW, time=300 min and initial effluent pH, for different temperatures.

The greatest COD reductions were obtained for H_2O_2 values of between 0.02-0.04 mol L^{-1} at 15 °C. Similar values were obtained by GilPavas et al. [37] for a real textile effluent from a factory in Medellin (Colombia) using Fe° and H_2O_2 at pH=3, and a comparable behavior was observed when the H_2O_2 concentration increases above 0.03 mol L^{-1}, where a lower COD reduction (%) value was obtained (from 76% to 65%).

Initially, increasing the dose of H_2O_2 increased the production of HO• available to attack the organic molecules, causing an increase in COD reduction (%). However, as the initial concentration of the oxidant increased, the HO• was consumed by the H_2O_2 (limiting reagent) to form a less reactive radical (HO_2•), Equation 1 [19]. HO_2• can be formed, in turn, when an excess of H_2O_2 reacts with Fe^{3+} [37].

$$H_2O_2 + HO^\bullet \rightarrow HO_2^\bullet + H_2O \qquad \varepsilon_{HO_2^\cdot} = 1.7\,V \; < \varepsilon_{HO^\cdot} = 2.8\,V \qquad \text{Equation 1}$$

At high concentrations of H_2O_2, the self-decomposition of the hydrogen peroxide in H_2O and O_2 may ocurr [38].

The maximum Fe^{2+} was reached for 0.02-0.04 mol L^{-1} of H_2O_2 in coincidence with the maximum COD reductions. The minimum concentration of Fe^{2+} was obtained at the lowest temperatures (between 15 and 21 °C) after 300 min. Similar results were observed in oxidation treatments of organic pollutants in wastewater [39-42].

3.1.2. Effect of CSW mass content.

The results obtained for the degradation of the effluent by varying the amount of added CSW between 0.0 and 0.4 g L^{-1}, maintaining the initial H_2O_2 concentration at 0.04 mol L^{-1} and using the initial pH of the effluent, are shown in Figures 4 a and b.

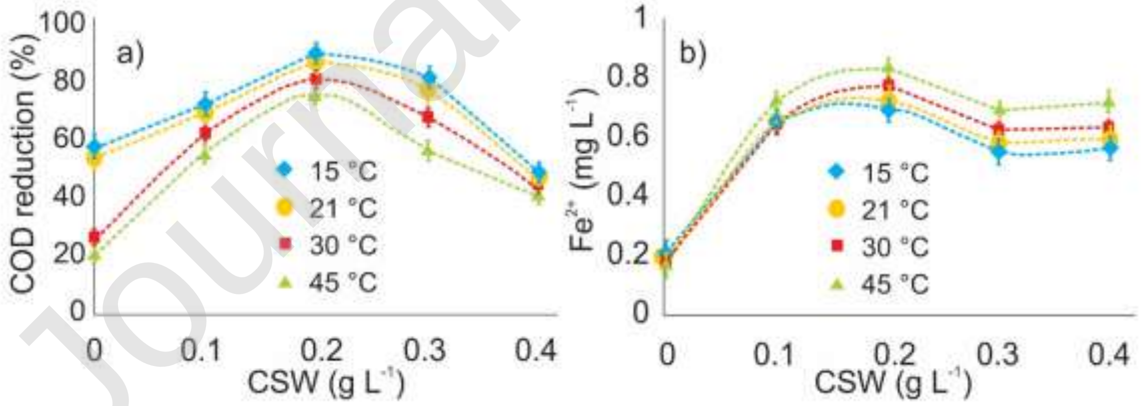

Figure 4. Effects of CSW mass content at 300 min for different temperatures on **a)** COD reduction (%), and **b)** Fe^{2+} concentration. Initial experimental conditions: $[H_2O_2]$=0.04 mol L^{-1} and initial pH of the effluent.

In previous works, the amounts of Fe° initially used for the treatment were larger. GilPavas et al. [37] and Segura et al. [43] analyzed a range between 2-9 g L^{-1} of Fe zero-valent, obtaining similar degradations to those reported in this work. The effect of CSW at low concentrations has received little study in previous reports [44].

The highest degradations were obtained for a CSW concentration of 0.2 g L^{-1}. For lower CSW values (between 0 and 0.2 g L^{-1}), COD reduction (%) increased up to a maximum value for all the tested temperatures. This could be due to the consumption of Fe^{2+} to generate HO• (Equation 2), leading to higher COD reductions. On the other hand, for concentrations greater than 0.2 g L^{-1}, it is evident that the amount of Fe^{2+} in the solution decreased, which could be attributed to the fact that at high concentrations of Fe^{2+} the trapping of HO• radicals would occur (Equation 3), generating a decrease in COD reduction.

$$Fe^{2+} + H_2O_2 \rightarrow Fe^{3+} + \mathrm{HO}\bullet + HO^- \qquad \text{Equation 2}$$

$$HO^{\bullet} + Fe^{2+} \rightarrow Fe^{3+} + HO^- \qquad \text{Equation 3}$$

$$\mathrm{Fe^0 + H_2O_2 \rightarrow Fe^{2+} + 2HO^-} \qquad \text{Equation 4}$$

In the absence of CSW, the initial amount of Fe^{2+} in the effluent was of 0.18 mg L^{-1} (Figure 4b). In Figure 4a it can be seen that this decrease in the initial Fe^{2+} concentration possibly favors the decomposition of H_2O_2 compared to HO• formation. This effect was more marked at higher temperatures.

3.2. Kinetic study: laboratory scale.

The kinetic study was carried out by measuring COD reduction. In a previous work, a central composite design with a 2^3 factorial design with added center points and star points was developed [33]. The input variables were oxidant concentration (0.002-0.08 mol L^{-1}), amount of CSW (0.02-0.4 g L^{-1}) and temperature (15-45 °C). COD reduction (%) was the response variable of the experimental design. The objective was to obtain the optimal values of the variables and their interactions. The optimum degradation conditions of the textile effluent were 0.037 mol L^{-1} of H_2O_2 and 0.247 g L^{-1} of CSW [33].

The concentration of Fe^{2+}, Fe^{3+} and pH were measured during the degradation process. An increase in % COD reduction was achieved with an increase in treatment time, whereas increasing temperature disfavored the degradation process (Table 1).

Table 1. Values of COD reduction (%) as a function of time for the optimum degradation conditions ($[H_2O_2]$ = 0.037 mol L^{-1} and 0.247 g L^{-1} of CSW) at different temperatures.

	COD reduction (%)			
Time (min)	**15.5 °C**	**21.0 °C**	**30.0 °C**	**45.0 °C**
0	0.00	0.00	0.00	0.00
60	37.31±1.06	25.65±0.99	18.57±1.08	21.82±0.93
120	56.90±0.78	47.57±1.19	41.32±0.73	35.28±1.34
180	69.03±0.98	64.37±1.01	53.85±0.90	47.82±0.83
240	82.56±1.15	75.09±0.80	68.71±1.39	63.60±0.58
300	87.69±0.90	85.82±0.28	80.32±1.02	75.21±0.67

The experimental results (Table 1) were modeled with pseudo-first order kinetics, through the COD parameter. The values of k_{deg} were calculated from the slope obtained from the representation of -ln (COD_f / COD_i) vs t.

The highest value of k_{deg} was obtained at 15 °C. To achieve a COD reduction (%) higher than 75% for temperatures between 15 °C and 21 °C, a treatment of over 200 min is required (effluent suitable for sewage discharge, COD value < 700 mg L^{-1}), whereas for temperatures of 30 °C and 45 °C, the treatment time should be at least of 300 min, showing the dependence of k_{deg} on temperature. These tests were performed in duplicate, obtaining the k_{deg} values shown in Table 2.

Table 2. k_{deg} values for different temperatures under optimal conditions ($[H_2O_2] = 0.037$ mol L^{-1}, 0.247 g L^{-1} of CSW, final time=300 min)

Temperature (°C)	**k_{deg} (min^{-1}) x10^3**	**R^2**
15	6.9±0.32	0.9954
21	6.4±0.41	0.9896
30	5.4±0.42	0.9825
45	4.5±0.50	0.9789

The values of k_{deg} were very similar in the temperature range studied. All tests ended when the concentration of residual hydrogen peroxide was of less than 20 mg L^{-1}, or when the degradation remained constant throughout the assay (after 300 min). The obtained rate constant values are similar to those reported by Behrouzeh et al. [40] for a homogeneous Fenton system in a pharmaceutical effluent and by Hou et al. [41] for a Fenton treatment system in a simulated textile effluent.

At the optimal concentrations of CSW and H_2O_2 (0.247 g L^{-1} and 0.037 mol L^{-1}, respectively) at 15.5 °C, the degradation could be monitored by TOC analysis. The reaction kinetics obtained by measuring TOC is shown in Figure 5.

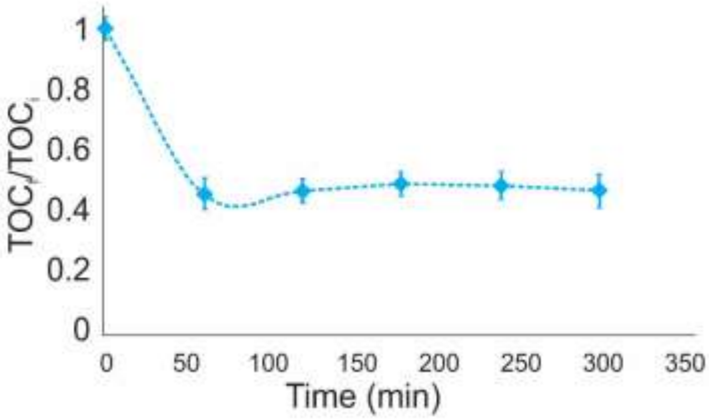

Figure 5. Kinetics of the degradation process by measuring TOC at 15 °C, experimental conditions: 0.037 mol L^{-1} of H_2O_2 and 0.247 g L^{-1} of CSW.

It can be observed that the degradation profile of the effluent reached TOC reduction values (%) close to 53% after 60 min of treatment. It should be noted that there is an important difference between the results obtained by TOC measurements and those obtained by COD measurements. Since the COD technique is based on the oxidation of all species that are able to be oxidized, the difference can be attributed to the presence of non-organic oxidizable species in the real effluent.

3.2.1. Fe^{2+} concentration vs. treatment time

Figure 6 a shows the maximum peak of Fe^{2+} at 50 min of treatment, which then decreased progressively until 300 min. This trend was observed for the different tested temperatures. The highest concentration of Fe^{2+} (1.91 mg L^{-1}) was obtained for temperatures between 15-21 °C. In the degradation reaction Fe^{2+} is consumed with the H_2O_2, giving rise to the production of HO• (Equation 2).

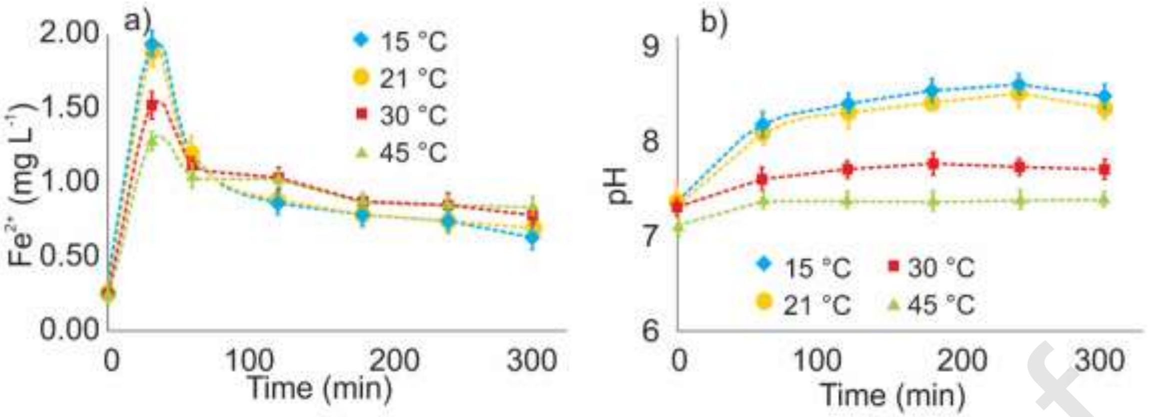

Figure 6. Graphical representation of **a)** Fe^{2+} concentration vs time; **b)** pH vs treatment time for different temperatures. Initial experimental conditions: $[H_2O_2] = 0.037$ mol L^{-1} and 0.247 g L^{-1} of CSW.

After 60 min of reaction, there was a decrease in the amount of Fe^{2+} in solution, and consequently a higher production of HO•.

The concentration of Fe^{2+} was lower with increasing temperature. Thus the system had excess of H_2O_2 and this produced an entrapment of HO•, resulting in a lower COD reduction (%). The total soluble Fe concentration for the different treatment temperatures was measured. In all cases, its value was below 2 mg L^{-1}, complying with Argentine regulations (Res. 336/2003) that establish a maximum limit of 10 mg L^{-1} of total soluble Fe for effluents to be discharged to the sewer. As the degradation time increased, the concentration of Fe^{3+} in the system increased up to 70% (0.83 mg L^{-1}, at 300 min).

3.2.2. pH vs treatment time

As it can be seen in Figure 6 b, the pH increased with increasing time of the degradation process. The reactions that occurred over time provided OH^- ions (Equations 1, 2, 3), so the pH increased throughout the treatment. A decrease in temperature produced an increase in pH, always within the parameters established by Resolution 336/03.

3.3. Behavior of the CSW surface during treatment

A sequence of micrographs of the CSW at different times of the degradation process were obtained. An oxide layer covering the surface of the CSW was observed after 180 min of reaction (Figure 7).

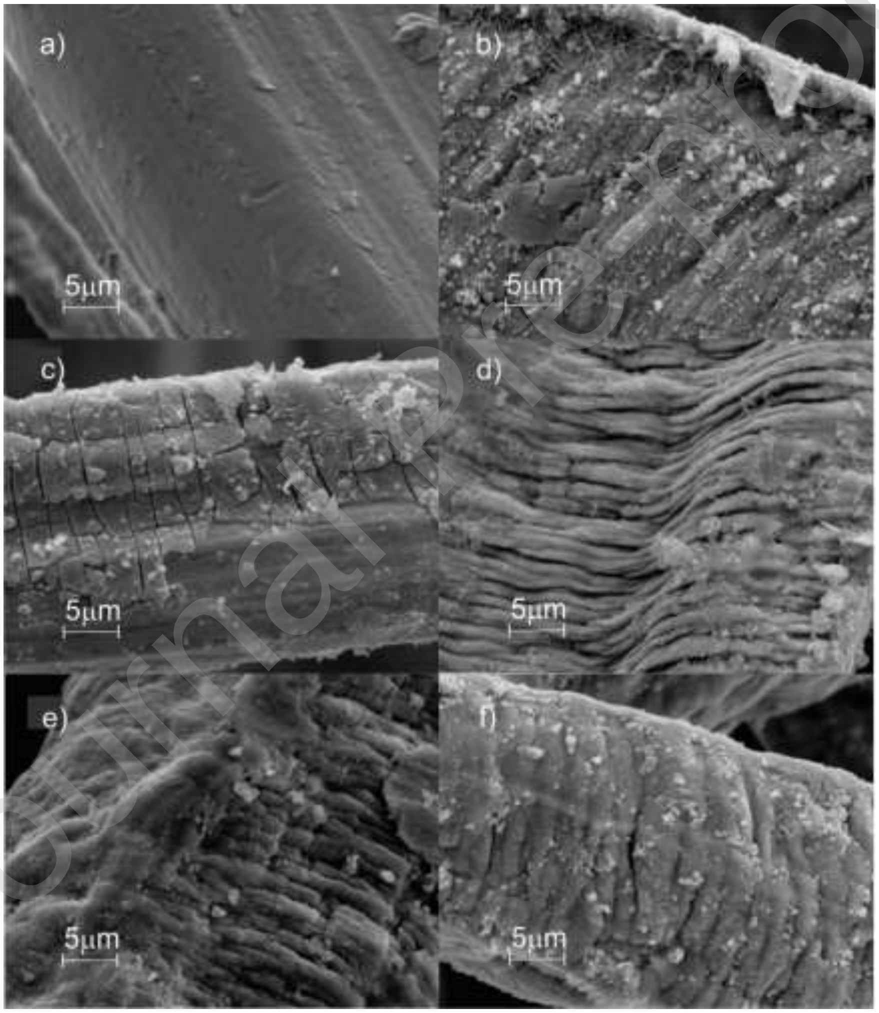

Figure 7. Micrographs of the CSW surface under optimum conditions ([H_2O_2] = 0.037 mol L^{-1}, 0.247 g L^{-1} of CSW and 15.5 °C), at 2000X magnification, 25 kV, at different treatment times: **a)** 0 min, **b)** 60 min, **c)** 120 min, **d)** 180 min, **e)** 240 min, and **f)** 300 min.

The concentration of Fe^{2+} decreased with increasing treatment time, which is in agreement with the micrographs showing only a small oxide layer between 0 and 60 min, allowing a contribution of Fe^{2+} to the system. Then there was an increase in the oxide layer over the reaction (Figure 7), without a significant production of ions.

The maximum peak of Fe^{2+} concentration was observed in the first hour of treatment, when the CSW surface did not present a uniform coverage, and in some areas the surface could be seen without any oxide layer.

3.4. Kinetic study: pilot scale.

A pilot test using a batch system of 5 L at 15 °C was carried out. The parameters monitored during the pilot experiments were COD reduction (%), pH, temperature, and Fe species in solution as a function of treatment time.

A COD reduction of 35% was obtained for a treatment time of 30 min, and of 68.5% for a treatment time of 300 min under the same laboratory-scale optimal conditions. The k_{deg} obtained at 300 min of treatment was of 0.0035 min^{-1} for conditions of 0.037 mol L^{-1} H_2O_2 and 0.247 g L^{-1} CSW at *ca.* 15 °C. The k_{deg} value at pilot scale was half of that obtained at laboratory scale (k_{deg}= 0.0065 min^{-1}) for a treatment time of 300 min at the same temperature (Figure 8).

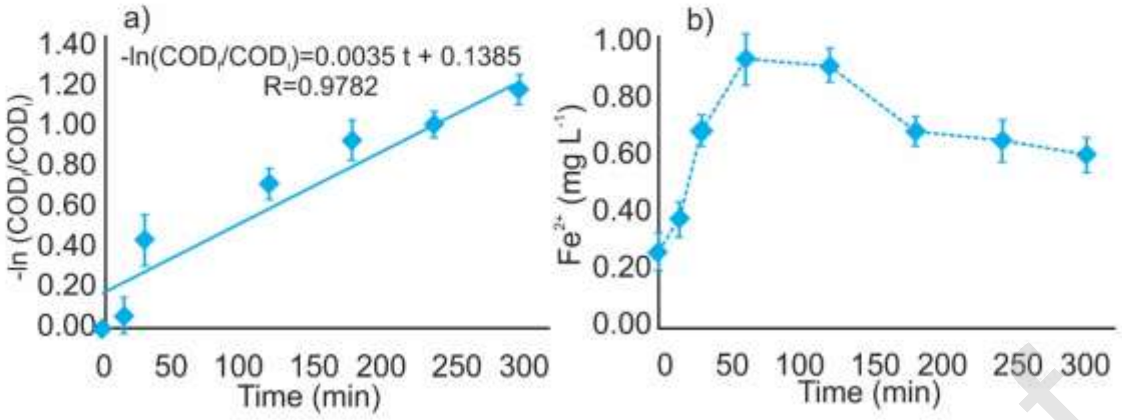

Figure 8. Plots of: **a)** -ln (COD_f/COD_i) vs time, **b)** Fe^{2+} concentration vs time, for optimal laboratory conditions at pilot scale. Conditions: 0.037 mol L^{-1} H_2O_2 and 0.247 g L^{-1} CSW at room temperature.

After 90 min of treatment, a maximum of 0.93 mg L^{-1} of Fe^{2+} was observed (Figure 8), and at 300 min a concentration of 0.60 mg L^{-1} was reached, with 35% of Fe^{2+} being consumed in the degradation process. The maximum amount of Fe^{2+} in the pilot test was lower than the Fe^{2+} concentration in the laboratory test. This caused a decrease in the production of HO•, and therefore a lower COD reduction (%) for the same treatment times. By decreasing the concentration of Fe^{2+}, H_2O_2 remains in excess, which leads to a faster decomposition of H_2O_2 and thus to a lower degradation rate.

The pH values were evaluated at different treatment times, observing an increase to up to 8.51 due to the reactions that lead to the degradation of the effluent. Another controlled parameter was system temperature as a function of time, obtaining a variation of 3 °C (from 13.4 to 16.5 ° C) after 420 min of treatment.

3.4.1. Process efficiency

The change in scale of the treatment is associated with an efficiency that will be used to recalculate the treatment times at industrial scale. This efficiency was determined experimentally by laboratory and pilot scale experiments conducted under the same experimental conditions. To obtain a COD value of 529.33 $mgO_2\ L^{-1}$, a reaction time of 178 min was needed at laboratory scale and of 240 min at pilot scale, and thus the efficiency value was calculated (Equation 5).

$$\varepsilon = \frac{\text{Treatment time at laboratory scale}}{\text{Treatment time at pilot scale}} \times 100 = 74.16\ \% \qquad \text{Equation 5}$$

3.5. Treatment optimization. Pulsed H_2O_2 and compact CSW

Adding the oxidant in pulses has the purpose of stabilizing its concentration in the medium and favoring the efficiency of the process [1]. The influence of the addition of H_2O_2 in pulses (5 fractions of 2 mL every hour) was studied. The CSW was used in a fixed bed. This set up exhibited a greater COD reduction (%) and its use would be more efficient when designing the treatment at industrial scale.

A COD reduction of 89.55% was obtained for a treatment time of 300 min. The experimental results were adjusted with pseudo-first order kinetics, obtaining a k_{deg} value of 0.0068 min^{-1} for 300 min of treatment (Figure 9 a).

Figure 9 b shows the concentration of Fe^{2+} as a function of treatment time. The maximum concentration of Fe^{2+} was 1.12 mg L^{-1} at 15 min under optimal operating conditions. This Fe^{2+} concentration was similar to that measured in the laboratory scale test

(1.16 mg L^{-1}). However, an increase in Fe^{2+} was observed at 120 and 240 min when pulsed H_2O_2 was added. These increases led to greater degradation rates.

The representation of pH as a function of time is shown as the degradation reaction proceeds (Figure 9 d), where there is an increase in pH to up of 8.74 at 400 min according to the degradation reactions. This parameter is within the range established by regulations for the disposal of wastewaters.

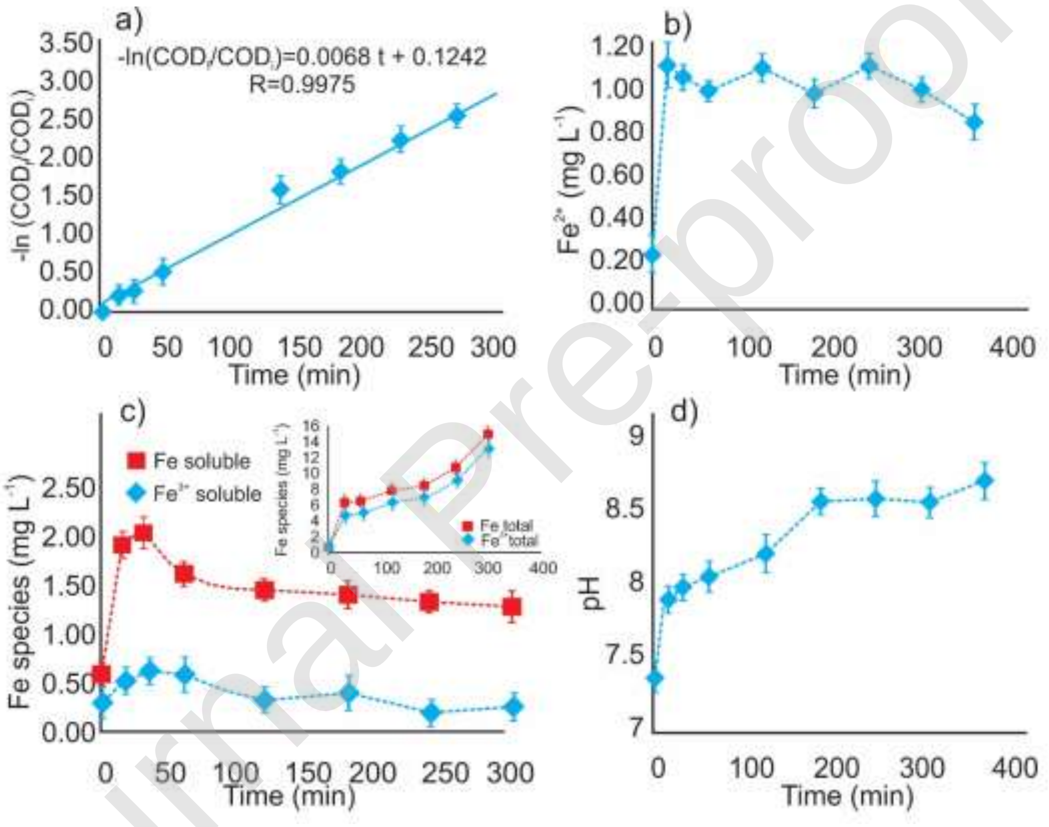

Figure 9. Plots of: **a)** -ln (COD_f / COD_i) vs time, **b)** concentration of Fe^{2+} vs time, **c)** concentration of Fe species in solution vs time, **d)** pH vs time, for pulsed H_2O_2 (5 fractions of 2 mL) and compact CSW at pilot scale.

Current legislation sets a maximum limit of 10 mg L^{-1} of soluble Fe_{total} for the discharge of effluents to the sewer. At 300 min of treatment, the concentration of soluble Fe_{total} was of 1.27 mg L^{-1} for the pilot study. The non-soluble Fe_{total} is *ca.*15 mg L^{-1} (Figure

9 c), which results in 3.7 kg of solids accumulating in each treatment, so it is necessary to incorporate a sludge elimination phase in the design of the treatment system.

The temperature of the system was evaluated as a function of time, with a variation of 5.5 °C (from 11.8 °C to 17.3 °C) for 300 min of treatment.

In Figure 10 a flow diagram of the different steps of the proposed degradation process is presented. As can be seen the process consist in three stages: (1) Coagulation-flocculation, (2) AOT: CSW/H_2O_2 treatment and (3) sedimentation-separation before final disposal or discharge.

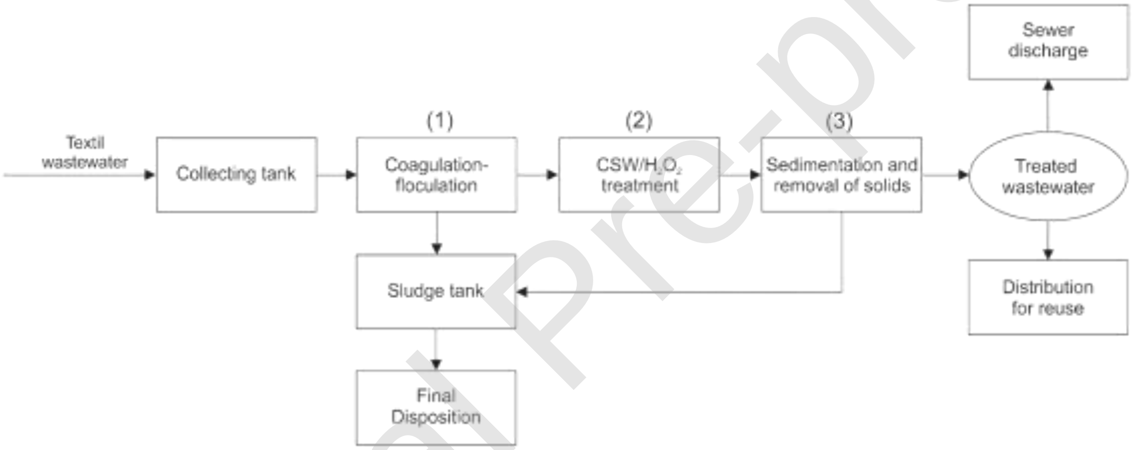

Figure 10. Flow chart of treatment of real non-biodegradable wastewater plant.

3.6. Phytotoxicity tests

Different concentrations (12.5, 25 and 100%) of untreated textile effluent (T0) and textile effluent treated for 300 min under optimal degradation conditions (T1) were used for the tests. The application of the treatment did not have negative effects on the germinative power (GP) of the seeds compared to the untreated effluent. No significant differences in root elongation were observed between the samples and the control with distilled water (See table 3).

The relative growth index (RGI) of the radicles of the lettuce and radish seedlings that grew from the seeds exposed to different effluent concentrations was determined. RGI was calculated as the ratio of the radicle length of the treated plants to the radicle length of the plants exposed to sterile distilled water.

Table 3. GP and RCI average values for lettuce and radish roots exposed to different concentrations of textile effluent.

Treatment	**RGI**		**GP (%)**	
	Lettuce	**Radish**	**Lettuce**	**Radish**
Control	0.80	0.80	98	98
T0-100	0.79±0.02	2.38±0.16	80±1.41	98±0
T0-25	1.17±0.06	2.35±0.14	87±0.71	93±0
T0-12.5	1.26±0.03	2.47±0.11	92±3.54	93±1.41
T1-100	0.72±0.06	2.33±0.06	83±5.66	93±2.83
T1-25	1.10±0.04	2.66±0.10	88±4.24	98±0
T1-12.5	1.14±0.03	2.52±0.13	87±3.54	100±0

Values above 0.8 indicate that there was no toxic effect. In the plates with radish seeds, a clear stimulation of root elongation with respect to the control was observed for all the tested concentrations. These results are in agreement with a previous report in which phytotoxicity tests were carried out on lettuce, evaluating germination and root elongation employing treated effluents [45].

3.7. Behavior of metallurgical waste as iron source

The waste from a turning facility (metallurgical waste) was used as a source of iron in equal proportions as the CSW. First the waste was characterized, and then its properties were evaluated.

It was observed that the metallurgical waste had a high surface content of Fe, even higher than that observed for the CSW (Figure 11), and traces of Cr, Si and Mn were also detected.

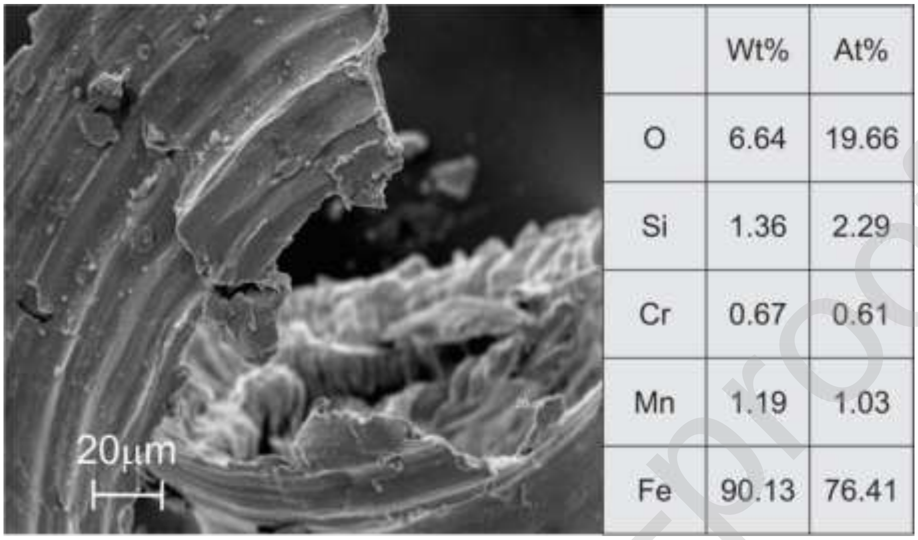

	Wt%	At%
O	6.64	19.66
Si	1.36	2.29
Cr	0.67	0.61
Mn	1.19	1.03
Fe	90.13	76.41

Figure 11. SEM micrograph at 250x magnification (20 kV) and EDS elemental analysis of the metallurgical waste.

The waste was evaluated under the optimal conditions obtained for the CSW. The effects of treatment time on the reduction of COD (%) and Fe^{2+} at 60, 120, 180, 240 and 300 min are shown in Figure 12 a and b. The working temperature was 21 °C at lab-scale.

The maximum concentration of Fe^{2+} was 1.15 mg L^{-1} at 60 min under optimal operating conditions. This concentration was similar to that measured at laboratory scale (1.16 mg L^{-1}). The k_{deg} obtained at 300 min of treatment was 0.0034 min^{-1} for conditions of 0.037 mol L^{-1} of H_2O_2 and 0.247 g L^{-1} of metallurgical waste at room temperature (*ca.* 15 °C). A COD reduction of 65% was reached at 300 min of treatment, with this value being below the limit established by Argentine legislation. The use of metallurgical waste as iron source in the Fenton treatment would contribute to reducing the environmental impact of industrial wastes, and revalues metallurgical wastes as a material of technological application.

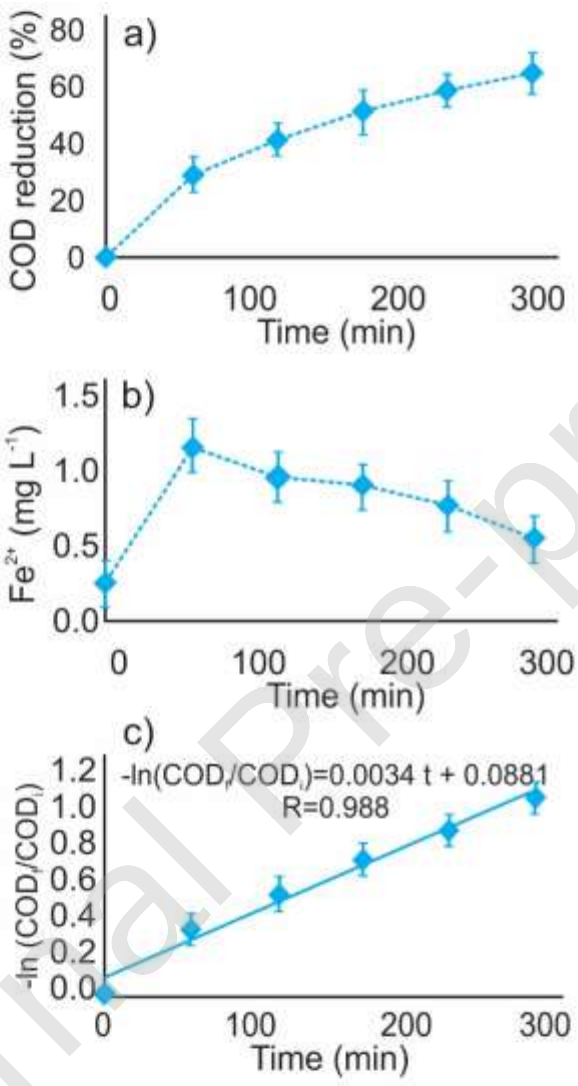

Figure 12. Graphical representation of **a)** COD reduction (%), **b)** Fe^{2+} vs treatment time, and **c)** –ln (COD_f/COD_i) vs time. Experimental conditions: 0.037 mol L^{-1} H_2O_2 and 0.247 g L^{-1} metallurgical waste at room temperature.

3.8. Costs and feasibility

3.8.1. Operating costs

The costs of the operation take into account the costs of the reagents needed to degrade the effluent under optimum conditions. Energy costs were not considered. The daily effluent flow is of 250 m^3 at industrial scale. Per day of treatment, the cost of H_2O_2 is U$S 852.00, and the cost of CSW is U$S 326.03. The total operation costs are U$S 1151.03 per day of treatment, that is U$S 0.32 per manufactured item of clothing.

Table 4. Summary of the costs.

Reagents				
H_2O_2		**CSW**		
Volume (L)	400	Quantity (Kg)	61.75	
U$S L^{-1}	2.13	U$S Kg^{-1}	5.26	
			U$S per day	**1151.03**
			U$S per m^3 of effluent	**4.6**
			U$S per item of clothing	**0.32**

The operating cost of 4.6 per m^3 of effluent is within the values reported by GilPavas et al. (2018) [45] and GilPavas et al. (2019) [37] (reported cost ranges from US$ 1.04 per m^3 to US$ 14.50 per m^3). Also, if the use of metallurgical waste as a replacement for CSW is taken into account, treatment costs can be reduced to U$S 3.4 per m^3 of effluent and the reuse of waste from another industry for the treatment of textile effluent is achieved.

3.8.2. Feasibility study

The textile effluent was degraded by 89.55% using CSW and H_2O_2 at pilot scale. A final COD value of 140.66 mgO$_2$ L^{-1} (the limit established by Argentine legislation is 700 mgO$_2$ L^{-1}) was obtained, thus the process is technically feasible. Industries in Argentina do not currently apply any additional treatment to effluents, but only a primary treatment by adding coagulant-flocculant to the wastewater. The application of the degradation treatment using CSW/H_2O_2 has an operating cost of U$S 4.6 per m^3 of effluent. The initial investment costs would be low because the proposed treatment would be coupled to the existing facilities of the textile company and use the design of the existing pools.

The degradation treatment turns the real textile effluent into a biodegradable wastewater (BOD_5/COD of 0.5 after the treatment), offering the possibility of performing a subsequent biological treatment to reuse the treated effluent in a production process. Previous studies on real textile effluents have reported increases in the BOD_5/COD ratio after the application of treatments with iron zero-valent and H_2O_2 [37, 43].

A phytotoxicity study was also carried out, where the treated effluent was found to be non-toxic under the studied conditions. The treated wastewater could be used as irrigation water or it could be discharged on land. These characteristics show that the proposed treatment is environmentally feasible. Another important factor is that the H_2O_2 used in the treatment is a "green" oxidant that does not affect the environment, and it was possible to measure that it was not present in the treated effluent.

4. Conclusions

In this study, the degradation of a real textile effluent was studied using hydrogen peroxide and commercial steel wool as source of iron. The effects of H_2O_2 concentration (0-0.04 mol L^{-1}), CSW mass (0-0.4 g L^{-1}), temperature (15-45 °C) and treatment time were studied. The maximum COD reduction (*ca.* 87%) was obtained for H_2O_2 of between 0.02-

0.04 mol L^{-1} and 0.2 g L^{-1} of CSW. Maximum Fe^{2+} was present within this concentration range, producing maximum % COD reduction. In the absence of H_2O_2, COD reduction was not significant. In the absence of CSW, the degradation was of *ca.* 20% due to the presence of Fe^{2+} in the initial wastewater.

The degradation kinetics was investigated at laboratory and pilot scale. The kinetic study was carried out by measuring COD reduction. The optimum degradation conditions of the textile effluent were 0.037 mol L^{-1} of H_2O_2, 0.247 g L^{-1} of CSW and temperature of 15 °C. At laboratory scale, COD reduction was of 87.6% in 300 min, reaching a discharge COD value of 188.5 mgO_2 L^{-1}. When CSW was replaced by a metallurgical residue, a reduction of 65% was obtained, reaching the discharge value (518.9 mgO_2 L^{-1}). The use of a metallurgical waste as iron source is a feasible option and contribute a great value to the work.

The treatment system can be optimized at pilot scale, achieving higher degradation rate constants at laboratory scale (k_{deg}= 0.0069 min^{-1} at lab scale and k_{deg}=0.0035 min^{-1} at pilot scale). Considering an industrial scale, a configuration consisting of a fixed bed and the addition of H_2O_2 in pulses was designed. A COD reduction of 89.55% was achieved at 300 min of treatment (k_{deg}=0.0068 min^{-1}).

The surface of the CSW was studied by SEM and monitored throughout the treatment, obtaining the surface changes as a function of time. After 60 min of treatment, the surface was covered by oxide, which is attributed to the contact of Fe with H_2O_2 to yield Fe^{2+}. On the other hand, the application of the proposed treatment process could be carried out at the industrial level considering that the cost of treatment would increase the cost per garment produced by only US $ 0.32. In addition, this cost is reduced by 26% if the metallurgical waste is used. The possible implementation reuse system of treated effluent would lead to a reduction in wastewater volumes and therefore in operating costs.

This study referring to the kinetic behavior of the different variables involved in the proposed process provides an essential tool for making decisions at different stages of the process attending to the possible variability in the physicochemical characteristics of the effluent.

Phytotoxicity tests were performed before and after treatment, showing that the effluent treated under optimal conditions was non-toxic. The CSW/H_2O_2 degradation process is an economically viable and environmentally friendly option.

Credit author statement

Pamela Belén Ramos: Investigation, Conceptualization, Methodology, Writing- Original draft preparation.

Paula Vitale, Investigation, Reviewing and Editing, Formal analysis

Gastón Pablo Barreto: Supervision, Reviewing

Francisca Aparicio: Investigation, Reviewing

María de los Ángeles Dublan, Investigation, Reviewing

Gladys Nora Eyler, Reviewing

Declaration of interests

The authors declare that they have no known competing financial interests or personal relationships that could have appeared to influence the work reported in this paper.

Acknowledgements

The authors thank Prof. Viviana Colasurdo for helping in the preparation of the characterization of the textile effluent, Melisa Tonetto for the language editing, and Dr. Daniel Mártire for his help and kindness.

Funding

This study was supported by the Engineering Faculty, the Secretary of Science, Art and Technology of the National University of the Center of the Province of Buenos Aires (SECAT-UNCPBA; subsidy INMAT 2016-2018), the National Council of Scientific and Technological Research (CONICET; PIP 11220150100844CO) and the Commission of Scientific Research of the province of Buenos Aires (CICPBA; 2157-584/2013-0). The phytotoxicity analyses were supported by the Faculty of Agronomy (UNCPBA). Pamela Belén Ramos is a postdoctoral fellowship holder of the CONICET. Paula Vitale is a postdoctoral fellowship holder of the CONICET. Gaston Pablo Barreto is a researcher of CONICET. Gladys Nora Eyler is a researcher of CICPBA. F. Aparicio thanks CONICET for her research graduate grant. María de los Ángeles Dublan is a researcher of UNCPBA.

References

[1] J. Blanco, F. Torrades, M. De la Varga, J. García-Montano, Fenton and biological-Fenton coupled processes for textile wastewater treatment and reuse, Desalination 286 (2012) 394–399. doi:10.1016/j.desal.2011.11.055.

[2] M. Sun, W. Huang, H. Cheng, J. Ma, Y.Kong, S. Komarneni, Degradation of dye in wastewater by Homogeneous Fe(VI)/$NaHSO_3$ System, Chemosphere 228 (2019) 595-601. doi: 10.1016/j.chemosphere.2019.04.182.

[3] J.J. Pignatello, E. Oliveros, A. MacKay, Advanced oxidation processes for organic contaminant destruction based on the Fenton reaction and related chemistry, Environ. Sci. Technol. 36 (2006) 1–84.doi: 10.1080/10643380500326564.

[4] A.M. Sales Solano, C.K. Costa de Araujo, J. Vieira de Melo, J.M. Peralta-Hernandez, D. Ribeiro da Silva, C.A. Martinez-Huitle, Decontamination of real textile industrial effluent by strong oxidant species electrogenerated on diamond electrode: Viability and disadvantages of this electrochemical technology, Appl. Catal. B-Environ. 130–131 (2013) 112–120. doi:10.1016/j.apcatb.2012.10.023.

[5] H. Yukseler, N. Uzal, E. Sahinkaya, M. Kitis, F.B. Dilek, U. Yetis, Analysis of the best available techniques for wastewaters from a denim manufacturing textile mill, J. Environ. Manage. (2017) 1118-1125. doi:10.1016/j.jenvman.2017.03. 041.

[6] I. Arslan-Alaton, G. Tureli, T. Olmez-Hanci, Treatment of azo dye production wastewaters using Photo-Fenton-like advanced oxidation processes: Optimization by response surface methodology, J. Photoch. Photobio A. 202 (2009) 142–153. doi:10.1016/j.jphotochem.2008.11.019.

[7] F. Torrades, J. García-Montaño, Using central composite experimental design to optimize the degradation of real dye wastewater by Fenton and photo-Fenton reactions, Dyes and Pigments 100 (2014) 184-189. doi:10.1016/j.dyepig.2013.09.004.

[8] P.R. Gogate, A.B. Pandit, A review of imperative technologies for wastewater treatment I: oxidation technologies at ambient conditions, Adv. Environ Res. 8 (2004) 501–551. doi:10.1016/S1093-0191(03)00032-7.

[9] L. Bilińska, M. Gmurek, S. Ledakowicz, Comparison between industrial and simulated textile wastewater treatment by AOPs – biodegradability, toxicity and cost assessment, Chem. Eng. J. 306 (2016) 550–559. doi:10.1016/j.cej.2016.07.100.

[10] X. Domènech, W.F. Jardim, M.I. Litter, Capitulo 1: procesos avanzados de oxidación para la eliminación de contaminantes, in: M.A. Blesa (Ed.), Programa Iberoamericano de Ciencia y Tecnología Para El Desarrollo (CYTED), CYTED, La Plata, 2001: pp. 3–25.

[11] K. Paździora, L. Bilińskab, S. Ledakowicz, A review of the existing and emerging technologies in the combination of AOPs and biological processes in industrial textile wastewater treatment, Chem. Eng. J. 376 (2019) 120-597.doi:10.1016/j.cej.2018.12.057.

[12] I. Oller, S. Malato, J. A. Sánchez-Pérez, Combination of Advanced Oxidation Processes and biological treatments for wastewater decontamination a review, Sci. Total Environ. 409 (2011) 4141–66. doi:10.1016/j.scitotenv.2010.08.061.

[13] S.G. Getinkaya, M.H. Morcali, S. Akarsu, C.A. Ziba, M. Dolaz, Comparison of classic Fenton with ultrasound Fenton processes on industrial textile wastewater, Sustain. Environ. Res. 28 (2018) 165-170. doi:10.1016/j.serj.2018.02.001.

[14] M.C.M. Ribeiro, M.C.V.M. Starling, M.M.D. Leao, C.C. De Amorim, Textile wastewater reuse after additional treatment by Fenton's reagent, Environ. Sci. Pollut. Res. 24 (2017) 6165–6175. doi:10.1007/s11356-016-6921-9.

[15] M. Taran, Utilization of petrochemical wastewater for the production of poly(3-hydroxybutyrate) by Haloarcula sp. IRU1, J. Hazard. Mater. 188 (2011) 26–8. doi:10.1016/j.jhazmat.2011.01.036.

[16] V. Pawar, S. Gawande, An overview of the Fenton Process for Industrial Wastewater, J. Mechan. Civ. Eng. (2015) 127–136.

[17] P. Xie, Y. Guo, Y. Chen, Z. Wang, R. Shang, S. Wang, J. Ding, Y. Wan, W. Jiang, J. Ma, Application of a novel advanced oxidation process using sulfite and zero-valent iron in treatment of organic pollutants, Chem. Eng. J. 314 (2017) 240–248. doi:10.1016/j.cej.2016.12.094.

[18] G.B. Ortiz de la Plata, O.M. Alfano, A.E. Cassano, 2-Chlorophenol degradation via photo Fenton reaction employing zero valent iron nanoparticles, J. Photochem. Photobiol., A. 233 (2012) 53– 59. doi:10.1016/j.jphotochem.2012.02.023.

[19] C.S.D. Rodrigues, L.M. Madeira, R.A.R. Boaventura, Treatment of textile effluent by chemical (Fenton´s Reagent) and biological (sequencing batch reactor) oxidation, J. Hazard. Mater. 172 (2009) 1551–1559. doi:10.1016/j.jhazmat.2009.08.027.

[20] N. Wanga, T. Zheng, G. Zhang, P. Wang, A review on Fenton-like processes for organic wastewater treatment. J. Environ. Chem. Eng. 4 (2016) 762–787. doi:10.1016/j.jece.2015.12.016

[21] S-H. Changa, S-H. Chuang, H-C. Li, H-H. Liang, L-C. Huang. Comparative study on the degradation of I.C. Remazol Brilliant Blue R and I.C. Acid Black 1 by Fenton oxidation and Fe^0/air process and toxicity evaluation. J. Hazard. Mater. 166 (2009) 1279–1288. doi:10.1016/j.jhazmat.2008.12.042.

[22] N. Bougdour, A. Sennaoui, I. Bakas, A. AssabbaneExperimental evaluation of Reactive Yellow 17 degradation using UV light and iron ions activated peroxydisulfate:

efficiency and kinetic model, Sci. Technol. Mater. 26 (2018) 1-9. doi:10.1016/j.stmat.2018.07.002.

[23] J. Sendhil, P. Muniswaran, C.A. Basha, Real Textile Dye Wastewater Treatment by Electrochemical Oxidation : Application of Response Surface Methodology. Int. J. Chem Tech. Research. 7 (2013) 2681–2690.

[24] J.C. Garcia, J.L. Oliveira, A.E.C. Silva, C.C. Oliveira, J. Nozaki, N.E. de Souza, Comparative study of the degradation of real textile effluents by photocatalytic reactions involving UV/TiO_2/H_2O_2 and UV/Fe^{2+}/H_2O_2 systems, J. Hazard. Mater. 147 (2007) 105–10. doi:10.1016/j.jhazmat.2006.12.053.

[25] R.P. Barkul, M.K. Patil, S.M. Patil, V.B. Shevale, S.D. Delekar, Sunlight-assisted photocatalytic degradation of textile effluent and Rhodamine B by using iodine doped TiO_2 nanoparticles, J. Photochem. Photobiol. A Chem. 349 (2017) 138–147. doi:10.1016/j.jphotochem.2017.09.011.

[26] A. Khatri, M.H. Peerzada, M. Mohsin, M. White. A review on developments in dyeing cotton fabrics with reactive dyes for reducing effluent pollution. J. Cleaner Prod. 87 (2015) 50-57. doi: 10.1016/j.jclepro.2014.09.017.

[27] F. Feng, Z. Xu, X. Li, W. You, Y. Zhen, Advanced treatment of dyeing wastewater towards reuse by the combined Fenton oxidation and membrane bioreactor process, J. Environ. Sci. 22 (2010) 1657–1665. doi:10.1016/S1001-0742(09)60303-X.

[28] R. Saravanan, V.K. Gupta, V. Narayanan, A. Stephen, Visible light degradation of textile effluent using novel catalyst ZnO/γ-Mn_2O_3, J. Taiwan Inst. Chem. E. 45 (2014) 1910–1917. doi:10.1016/j.jtice.2013.12.021.

[29] V.J.P. Vilar, L.X. Pinho, A.M.A. Pintor, R.A.R. Boaventura, Treatment of textile wastewaters by solar-driven advanced oxidation processes, j. Sol. Energy. 85 (2011) 1927–1934. doi:10.1016/j.solener.2011.04.033.

[30] P.A. Soares, T.F.C.V. Silva, A. Ramos, S.M.A. Guelli, U. Souza, R.A.R. Boaventura, V.J.P. Vilar, Assessment of AOPs as a polishing step in the decolourisation of biotreated textile wastewater: technical and economic considerations, J. Photochem. Photobiol. A Chem. 317 (2016) 26–38. doi:10.1016/j.jphotochem.2015.10.017.

[31] F.L. Rosario-Ortiz, E.C. Wert, S.A. Snyder, 2010. Evaluation of UV/H_2O_2 treatment for the oxidation of pharmaceuticals in wastewater. Water Res. 44 (2010) 1440-1448. doi: 10.1016/j.watres.2009.10.031.

[32] P.B. Ramos, M.A. Bavio, G.P. Barreto, G.N. Eyler. Degradación de un efluente textil real asistida por Fe/PVA y materiales residuales magnéticos. Revista Matéria. 23 (2). (2018). doi: 10.1590/s1517-707620180002.0430.

[33] P.B. Ramos, P. Vitale, G.P. Barreto, G.N. Eyler. Tratamiento de efluente textil real mediante TAOs. IX CAIQ2017. AAIQ Asociación Argentina de Ingenieros Químicos. Bahía Blanca (2017).

[34] P.K. Tarafder, A.R. Thakur. An optimised 1,10-phenanthroline method for the determination of ferrous and ferric oxides in silicate rocks, soils and minerals. Geostand. Geoanal. Res. 37 (2013) 155–168, doi:10.1111/j.1751-908X.2012.00183.x.

[35] A.R. Navarro, R.G. Arrueta, M.C. Maldonado. Determinación del efecto de diferentes compuestos a traves de ensayos de fitotoxicidad usando semillas de lechuga, escarola y achicoria. Rev. Toxicol. 23 (2006) 125–129.

[36] B.J. Young, N.I. Riera, M.E. Beily, P.A. Bres, D.C. Crespo, A.E. Ronco. Toxicity of the effluent from an anaerobic bioreactor treating cereal residues on *Lactuca sativa*. Ecotox. Environ. Safe. 76 (2012), 182-186. doi: 10.1016/j.ecoenv.2011.09.019.

[37] E. GilPavas, S. Correa-Sanchez, D.A. Acosta. Using scrap zero valent iron to replace dissolved iron in the Fenton process for textile wastewater treatment: Optimization and assessment of toxicity and biodegradability, Environmental Pollution 252 (2019) 1709-1718. doi:10.1016/j.envpol.2019.06.104.

[38] L.B. De Lima, L.O. Pereira, S.G. de Moura, F. Magalhães, 2017. Degradation of organic contaminants in effluents synthetic and from the textile industry by Fenton, photocatalysis, and H_2O_2 photolysis. Environ. Sci. Pollut. Res. 24 (2017) 6299–6306.

[39] N. Ertugay, F.N. Acar, Removal of COD and color from Direct Blue 71 azo dye wastewater by Fenton's oxidation: Kinetic study. Arabian, Journal of Chemistry (2017) 10 1158–1163. doi:10.1016/j.arabjc.2013.02.009.

[40] M. Behrouzeh, M. Abbasi, S. Osfouri, M.J. Dianat. Treatment of DMSO and DMAC wastewaters of various industries by employing Fenton process: Process performance

and kinetics study. J. Environ. Chem. Eng. 8 (2020) 103-597.doi: 10.1016/j.jece.2019.103597.

[41] M.F. Hou, L. Liao, W.D. Zhang, X.Y. Tang, H.F. Wan, G.C. Yin, Degradation of rhodamine B by Fe(0)-based Fenton process with H_2O_2. Chemosphere 83 (2011) 1279–1283. doi:10.1016/j.chemosphere.2011.03.005.

[42] F. Ghanbari, M. Moradi. A comparative study of electrocoagulation, electrochemical Fenton, electro-Fenton and peroxi-coagulation for decolorization of real textile wastewater: Electrical energy consumption and biodegradability improvement. J. Environ. Chem. Eng. 3 (2015) 499–506. doi:10.1016/j.jece.2014.12.018.

[43] Y. Segura, F. Martinez, J.A. Melero, J.L.G. Fierro, Zero valent iron (ZVI) mediated Fenton degradation of industrial wastewater: Treatment performance and characterization of final composites. Chem. Eng. J., 269 (2015) 298–305. doi: 10.1016/j.cej.2015.01.102.

[44] A. Flores, P. Vitale, G.N. Eyler, A.I. Cañizo, Remoción de colorantes textiles aplicando procesos fotoquímicos oxidativos (UV/H_2O_2/lana de acero comercial), Afinidad: Revista de química teórica y aplicada, 72 (2015) 188-195.

[45] A. Priac, P-M. Badot, G. Crini, Treated wastewater phytotoxicity assessment using Lactuca sativa: Focus on germination and root elongation test Parameters, Comp. Rendus Biolog., 340 (2017) 188-194.

[46] E. GilPavas, I. Dobrosz-Gómez, M.A. Gómez-García, Optimization and toxicity assessment of a combined electrocoagulation H_2O_2/Fe^{2+}/UV and activated carbon adsorption for textile wastewater treatment, Sci. Total Environ. 651 (2019) 551–560. doi:10.1016/j.scitotenv.2018.09.125.

Table caption

Table 1. Values of COD reduction (%) as a function of time for the optimum degradation conditions ($[H_2O_2] = 0.037$ mol L^{-1} and 0.247 g L^{-1} of CSW) at different temperatures.

Table 2. k_{deg} values for different temperatures under optimal conditions ($[H_2O_2] = 0.037$ mol L^{-1}, 0.247 g L^{-1} of CSW, final time=300 min)

Table 3. GP and RCI average values for lettuce and radish roots exposed to different concentrations of textile effluent.

Table 4. Summary of the costs.

Figure caption

Figure 1. a) SEM micrograph of the surface of CSW at 200X magnification, 20 kV. **b)** X-ray diffractogram of CSW.

Figure 2. Schematic diagram of the pilot-scale experimental system with a CSW packed bed.

Figure 3. **a)** Effect of H_2O_2 concentration on COD reduction (%), experimental conditions: 0.2 g L^{-1} of CSW, time=300 min and initial effluent pH, **b)** Effect of H_2O_2 concentration on Fe^{2+} profiles, experimental conditions: 0.2 g L^{-1} of CSW, time=300 min and initial effluent pH, for different temperatures.

Figure 4. Effects of CSW mass content at 300 min for different temperatures on **a)** COD reduction (%), and **b)** Fe^{2+} concentration. Initial experimental conditions: $[H_2O_2]$=0.04 mol L^{-1} and initial pH of the effluent.

Figure 5. Kinetics of the degradation process by measuring TOC at 15 °C, experimental conditions: 0.037 mol L^{-1} of H_2O_2 and 0.247 g L^{-1} of CSW.

Figure 6. Graphical representation of **a)** Fe^{2+} concentration vs time; **b)** pH vs treatment time for different temperatures. Initial experimental conditions: $[H_2O_2]$ = 0.037 mol L^{-1} and 0.247 g L^{-1} of CSW.

Figure 7. Micrographs of the CSW surface under optimum conditions ($[H_2O_2]$ = 0.037 mol L^{-1}, 0.247 g L^{-1} of CSW and 15.5 °C), at 2000X magnification, 25 kV, at different treatment times: **a)** 0 min, **b)** 60 min, **c)** 120 min, **d)** 180 min, **e)** 240 min, and **f)** 300 min.

Figure 8. Plots of: **a)** -ln (COD_f/COD_i) vs time, **b)** Fe^{2+} concentration vs time, for optimal laboratory conditions at pilot scale. Conditions: 0.037 mol L^{-1} H_2O_2 and 0.247 g L^{-1} CSW at room temperature.

Figure 9. Plots of: **a)** -ln (COD_f / COD_i) vs time, **b)** concentration of Fe^{2+} vs time, **c)** concentration of Fe species in solution vs time, **d)** pH vs time, for pulsed H_2O_2 (5 fractions of 2 mL) and compact CSW at pilot scale.

Figure 10. Flow chart of treatment of real non-biodegradable wastewater plant.

Figure 11. SEM micrograph at 250x magnification (20 kV) and EDS elemental analysis of the metallurgical waste.

Figure 12. Graphical representation of **a)** COD reduction (%), **b)** Fe^{2+} vs treatment time, and **c)** –ln (COD_f/COD_i) vs time. Experimental conditions: 0.037 mol L^{-1} H_2O_2 and 0.247 g L^{-1} metallurgical waste at room temperature.